DOI: 10.13009/EUCASS2022-7245
9TH EUROPEAN CONFERENCE FOR AERONAUTICS AND SPACE SCIENCES (EUCASS)

High Altitude Rocket Reactive Jet Flow Simulations with a Hybrid NS-DSMC Methodology

Virgile Charton[⋆]*, Adrien Langenais*[⋆]*, Julien Labaune*[⋆†]
[⋆] *DMPE, ONERA, Université Paris Saclay*
F-91123 Palaiseau - France
virgile.charton@onera.fr · adrien.langenais@onera.fr · julien.labaune@onera.fr
[†]Corresponding author

Abstract

The present work uses a hybrid methodology to simulate a multispecies reactive flow expanding from a highly pressurized nozzle into a vacuum. The methodology couples Navier-Stokes resolution and Direct Simulation Monte Carlo in a one-way approach that enables the simulation of steady-state and quasi-steady-state problems. The idea is to split the calculation into zones where the flow is either computed by computational fluid dynamics resolving Navier-Stokes equations or by Direct Simulation Monte Carlo according to specific criteria based on the rarefaction level. Such methodology was experienced in the context of micro-thrusters exhausting a cold nitogen flow and optimized for highly pressurized thrusters in previous research work. The present work aims at improving the methodology and enabling the plasma simulation in the thruster plume. In this paper, the simulation of a metric-sized nozzle with multispecies reactive flow is carried out. A particular interest is the electron density resulting from ionization of the flow, answering a need for the prediction of radio communication attenuation between the ground station and the rocket. To that purpose, a complex chemistry scheme involving ions and electrons is post-computed from a baseline flow solution for which ionization is not natively considered. The rocket geometry and the flow characteristics such as the combustion chamber pressure and temperature and the considered species and chemical reactions are taken as close as possible to an actual configuration.

1. Introduction

The design of several aerospace systems involves studying multiscale physical phenomena. For example, high-altitude rocket propulsion, vehicle re-entry, atmospheric deceleration, landing or satellite propulsion typically encounter both high density and rarefied flows. Numerical simulation of such flows is a challenge. Classical Computational Fluid Dynamics (CFD) continuous approaches resolving Navier-Stokes (NS) equations are inaccurate in predicting rarefied regime flows where the Boltzmann equation may be considered. The Direct Simulation Monte Carlo method (DSMC) is widely used to solve the Boltzmann equation. However, the computational cost of DSMC increases significantly with the flow density. Thus, to accurately simulate rarefied as well as high-density areas of multiscale flows, a hybrid methodology that couples CFD and DSMC can be used. The idea is to split the calculation into zones where the flow is either computed by CFD or DSMC according to specific criteria based on the rarefaction level.

Several authors operate such hybrid multi-scale methods: Latorre *et al.* [1] performed numerical simulations of micro-satellite thruster flow expanding from a supersonic nozzle into vacuum; Ivanov *et al.* [2] studied satellite propulsion backflow that can cause contamination of the equipment such as solar panel or thermal control; Glass *et al.* [3, 4] and Deschenes *et al.* [5] simulated vehicles planetary re-entry to determinate aerodynamic coefficients, pressure and temperature distributions that are key parameters to design thermal protection or deceleration technology; Burt *et al.* [6] worked on rocket stage separation; Marichalar *et al.* [7] on lunar landing; Xu *et al.* [8] performed lightcraft laser propulsion simulations; Aktas *et al.* [9] investigated microfluidics phenomena. An outline of aerospace applications that require a multi-scale analysis can be found in the review of Boyd *et al.* [10].

Another application involving high-density variation flow is communication issues with ground stations during a rocket flight at a high altitude. This occurs due to the ionized exhaust plume of the engine that interferes with radio frequency transmission [11, 12]. Classical CFD continuous method gives good results at a flight altitude of 100 km and under, but, as showed by Kinefuchi *et al.* [13, 14], suffers low accuracy for higher altitudes where rarefied effects have to be considered. Accurate comprehension of the flow behaviour involving continuous and rarefied regimes is

DOI: 10.13009/EUCASS2022-7245

therefore needed to determine the correct flow extension and the associated electron distribution. Simulation of such flow is expensive regarding computational cost, even using a hybrid approach. Thus, the first step is to select a suited hybrid CFD-DSMC method.

A strategy was proposed in a previous work [15], where a one-way coupling methodology was used to reproduce the experimental results of a micro-thruster cold nitrogen flow realized at the German Aerospace Centre (DLR) Gottingen High-Vacuum Plume Test Facility for Chemical Thrusters (STG-CT) [16, 17]. In this previous work, the construction of the interface between continuous and rarefied flow was studied and optimized, allowing significant computational cost reduction. The present work aims at enhancing this methodology to simulate multispecies reactive flow with ionization and obtain the electron density field. Two main hypotheses are proposed to achieve this goal: firstly, the reaction mechanism is considered as frozen in the rarefied part of the flow as the temperature and pressure reach a very low level leading to fewer particles interactions; secondly, the flow expansion is supposed to be driven by the major species, and the influence of ions and electrons is negligible. The last hypothesis allows us to post-compute the minor species from the flow solution rather than natively calculate them, as handling such species in a DSMC simulation is complex. The required particle characteristics to model collision interactions are often hard or not possible to obtain. Moreover, free electrons computation using DSMC is complicated since they have a very high velocity regarding other species requiring a very small time step. The classical hypothesis to overcome this issue, such as ambipolar diffusion, is hardly applicable for plasma containing negative ions, which is the case in our work context. Hence, a possible way is to post-compute a more complex chemical kinetic scheme accounting for ions and electrons only along selected streamlines as it is done for asteroid entry simulations [18].

The case exploited in this paper is a steady-state simulation of the flow from a fictive rocket nozzle corresponding to 1/10th downscale of JAXA's M-V rocket third stage called M34b [14], at an altitude of 200 *km*. The effect of the atmosphere's rarefaction is shown by comparing the results between conventional NS and the hybrid NS-DSCM simulations. The paper is organized as follows: section 2 is dedicated to the presentation of the simulation methodology and the numerical tools used, section 3 presents the simulation results, and section 4 gives a discussion and conclusion about the methodology and the possible enhancement.

2. Numerical simulation methodology

2.1 Overview of the methodology and simulation cases

This section describes the hybrid NS-DSMC methodology used for this study. The definition of the interface between continuous and rarefied flow areas was studied and optimised in a previous study by the authors [15]. It is based on the breakdown parameter B described by Garcia *et al.* [19] which quantifies the rarefaction level of the flow according to local variations of the flow quantities. In the context of rocket thruster flow, the one-way coupling strategy assumes a supersonic flow along the interface between the continuous and rarefied areas. Thus, only the influence of NS outgoing toward DSMC area is considered as the flow moves from the continuous area to the rarefied one. The continuous and rarefied flow solutions are computed using only the major species produced by the combustion chamber and the associated reaction scheme. More complex chemistry is post-computed along the flow solution streamlines, giving the final electron density field. Figure 1 illustrates the two simulation areas, the interface between them and the streamlines along which complex chemistry is post-computed.

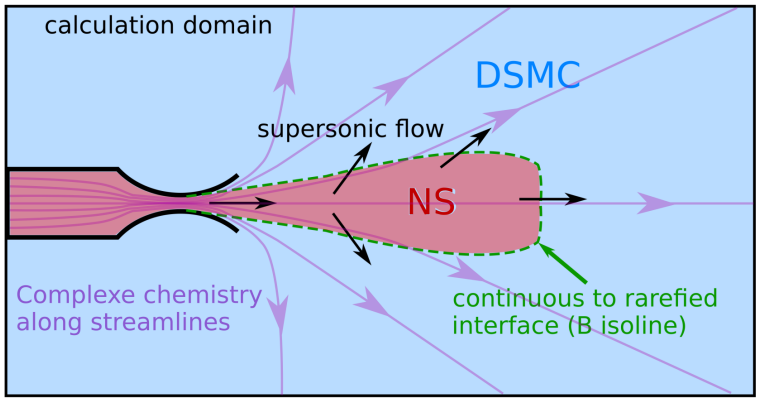

Figure 1: Scheme of the NS and DSMC calculation domains

DOI: 10.13009/EUCASS2022-7245

The methodology is composed of the following steps:

1. First, a NS simulation of the entire domain is performed. At this point, there is no distinction between rarefied and continuous areas. Thus, only the denser part of the flow solution is correct. However, this first simulation allows to calculate the local rarefaction level in the entire domain.
2. The rarefaction level is calculated using the breakdown criterion B with an additional truncation cut in the exit plane of the nozzle as described in [15]. The interface between continuous and rarefied areas is defined by a chosen B isoline and cannot enter the nozzle. Optimized B values in the context of highly pressurized thrusters are given in the previous authors' work, ranging from 0.05 to 0.2.
3. Once the interface is set, temperature, velocity and density values are extracted from the NS simulation along the isoline. The interface is composed of discrete segments for which extracted values are used to build distribution functions.
4. Next, a DSMC simulation is performed over the rarefied area. Each segment of the interface defined in the previous step acts as an inflow boundary condition, emitting particles according to the distribution functions.
5. Finally, streamlines are extracted from the flow solution over the continuous and rarefied areas, and the species concentrations are recomputed along them considering a more complex chemical kinetic scheme accounting for ions and electrons.

Figure 2 shows the nozzle geometry considered in this paper. It is a 1/10th downscale inspired by the JAXA's rocket M-V third stage called M34b [14, 20]. The combustion chamber diameter is 0.2229 m, the throat diameter is 0.0190 m, the exit diameter is 0.1863 m, the divergent length is 0.2414 m, and the combustion chamber length is 0.1863 m. There is no co-flow, and the nozzle is considered to be static. Hence, the flow is steady-state and is exhausted from the nozzle into a $p = 10^{-4}$ Pa vacuum, corresponding to the pressure encountered at an altitude of 200 km. The generation pressure and temperature characterizing the combustion chamber are $p_0 = 1.0$ bar and $T_0 = 3000$ K. The generation pressure is reduced compared to the full-scale engine pressure, which is 56.0 bar. The kinetic scheme involving the combustion product species are given in Troyes *et al.* [21], Jensen *et al.* [22, 23] and Plane *et al.* [24] works in which reactions in the gas mixture produced by solid propellant combustion are studied. The species mass fraction at the nozzle inlet, given in table 1, are evaluated at equilibrium considering a solid propellant comprised of hydroxy-terminated polybutadiene, 68% ammonimum perchlorate and 20% aluminium as the one used for M34b stage [20]. The 17 considered species are the following: N_2, H_2, O_2, H_2O, H, O, OH, CO, CO_2, HCl, Cl_2, Cl, Na, $NaCl$, Cl^-, Na^+, and e^-. The chemical mechanism of the gas mixture is given in table 2. In this work, the reactions are modeled with Arrhenius equations.

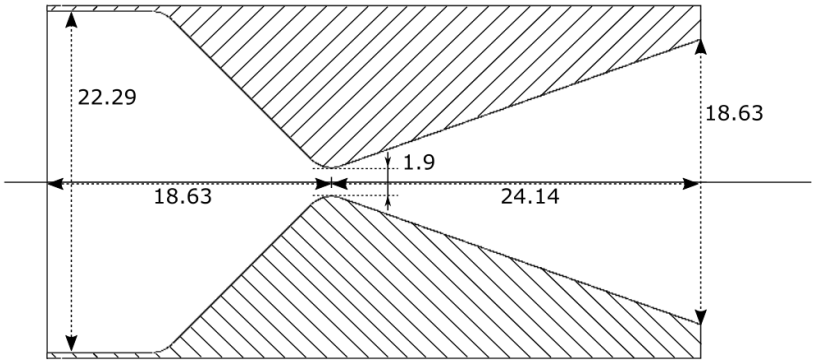

Figure 2: Nozzle geometry: 1/10th downscale of M34b nozzle of JAXA's M-V rocket third stage. Values are in centimetres

Two scenario cases are simulated in this paper. The first one, called NS full chemistry, corresponds to a NS simulation of the flow using table 2 kinetic scheme accounting for the 17 species, including ions and electrons, and the 24 reactions. The flow solution obtained from this first simulation does not account for rarefaction effects. It is used to compare the final solution of the hybrid methodology to the simple NS solution. The second simulation, called hybrid reduced chemistry, corresponds to the hybrid simulation of the flow without ions and electrons. Only 14 species are involved, N_2, H_2, O_2, H_2O, H, O, OH, CO, CO_2, HCl, Cl_2, Cl, Na, $NaCl$, and the kinetic scheme is composed of the 17 first reactions.

The tools and methods used at each step of the hybrid simulation are detailed in the following sections.

DOI: 10.13009/EUCASS2022-7245

$N2$	$H2$	$O2$	H_2O	H	O	OH
0.132789	0.036653	0.000142	0.124785	0.002246	0.000471	0.006997

CO	CO_2	HCl	Cl_2	Cl	Na	$NaCl$
0.378396	0.028127	0.26765	8.8e-05	0.021299	1.6e-05	0.000341

Table 1: Species mass fraction at the nozzle inlet, evaluated at equilibrium considering a solid propellant comprised of hydroxy-terminated polybutadiene, 68% ammonimum perchlorate and 20% aluminium

No	Reaction	Reference
1	$O_2 + H = O + OH$	[21]
2	$H_2 + O = H + OH$	[21]
3	$H_2 + OH = H_2O + H$	[21]
4	$OH + OH = H_2O + O$	[21]
5	$H + H + M = H_2 + M$	[21]
6	$H + OH + M = H_2O + M$	[21]
7	$H + O + M = OH + M$	[21]
8	$O + O + M = O_2 + M$	[21]
9	$OH + CO = H + CO_2$	[21]
10	$O_2 + CO = O + CO_2$	[21]
11	$O + CO + M = CO_2 + M$	[21]
12	$H + HCl = H_2 + Cl$	[21]
13	$H + Cl_2 = HCl + Cl$	[21]
14	$OH + HCl = H_2O + Cl$	[21]
15	$O + HCl = OH + Cl$	[21]
16	$Cl + Cl + M = Cl_2 + M$	[21]
17	$H + Cl + M = HCl + M$	[21]
18	$Cl + e^- + M = Cl^- + M$	[22]
19	$HCl + e^- = Cl^- + H$	[22]
20	$Na^+ + e^- + M = Na + M$	[23]
21	$Na^+ + Cl^- = Na + Cl$	[23]
22	$Na^+ + Cl^- + M = NaCl + M$	[23]
23	$Na + HCl = NaCl + H$	[24]
24	$Na + Cl + M = NaCl + M$	[24]

Table 2: Kinetic scheme of the simulated gas mixture issued from the propellant combustion. The third body M can be any of the species (excepted e^-) with an equal relative efficiency

2.2 Navier-Stokes simulation

In this study, Onera code CEDRE is used to resolve NS equations with a finite volume approach. This tool is a 3D multi-physics code [25] developed to realize numerical studies of energetics and propulsion fields both for research and industrial use. CEDRE can simulate complex flow involving reactive, compressible, multiphase, or radiative physics that can be encountered during solid or liquid rocket propulsion.

The nozzle geometry allows the use of an axial symmetry. The size of the simulation box is 17.5×40.0 m which is approximately a hundred times the nozzle size in the axial direction to ensure that the plume is fully simulated. The flow is considered to be laminar. Figure 3 presents the mesh used for the simulation. It is made of unstructured triangles and has approximately 800 000 cells. The y^+ values along the nozzle wall are in the desired range ($y^+ < 1$), so the near-wall mesh is fine enough to capture the viscous sublayer where a linear velocity law can be used.

The boundary conditions are defined as follows:

1. $p_0 = 1.0$ bar and $T_0 = 3000$ K are imposed at nozzle inflow, corresponding to the combustion chamber. The species generated by the propellant combustion are injected considering thermochemical equilibrium.

2. The nozzle wall condition is a Maxwell-Smoluchowski [26] condition with an accommodation coefficient set to 1 as proposed in [15]. Such condition allows to take into account the possible bounces on velocity and temperature in pseudo-rarefied areas during NS simulations, particularly in the boundary layer of the inner nozzle divergent

DOI: 10.13009/EUCASS2022-7245

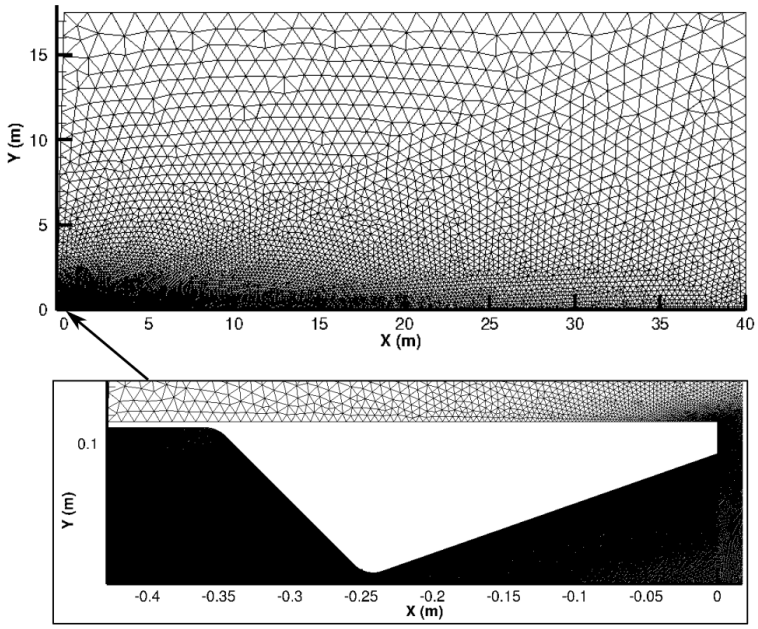

Figure 3: Unstructured mesh of NS simulation

wall. Moreover, the nozzle walls are considered as isothermal walls with a temperature of 2000 K for the inner wall and 287 K for the outer wall.

3. The outer right, left and top domain boundaries are defined as supersonic outflows with imposed $p = 10^{-4}$ Pa corresponding to the vacuum level encountered at 200 km of altitude.

4. The bottom domain boundary is set as an axial symetry axis.

2.3 Rarefaction level and interface between continuous and rarefied areas

An isocontour of rarefaction level is used to delimit two areas, one where the flow is considered continuous, and the other where it is rarefied. DSMC computational cost increases significantly with flow density, and the definition of the rarefaction criterion has great practical importance. There are multiple criteria in the literature, from the Knudsen number K_n to the breakdown parameter B introduced by Garcia *et al.* [19]. In this study, as in our previous study [15], B criterion is used to define the interface between continuous and rarefied flow areas. NS equations can be derived from Boltzmann's theory assuming only small deviations from local thermal equilibrium. This deviation introduces terms associated with heat flux q and shear stress τ. Consequently, their magnitudes indicate the degree of deviation from local thermodynamic equilibrium, which is interpreted in Garcia *et al.* parameter. B is defined as follows:

$$B = max(q_i, \tau_{i,j}) \tag{1}$$

with:

$$\begin{cases} q_i = -\dfrac{\kappa}{p}\left(\dfrac{2m}{k_B T}\right)^{1/2} \dfrac{\partial T}{\partial x_i} \\ \tau_{i,j} = \dfrac{\mu}{p}\left(\dfrac{\partial v_i}{\partial x_j} + \dfrac{\partial v_j}{\partial x_i} - \dfrac{2}{3}\dfrac{\partial v_k}{\partial x_k}\delta_{i,j}\right) \end{cases} \tag{2}$$

where μ and κ are respectively the dynamic viscosity and the thermal conductivity, k_B is the Boltzmann coefficient, and m is the particle's mass. One of our previous work's focuses was on optimising the B isoline value to simulate accurately highly pressurised thrusters using a hybrid NS-DSMC methodology. It has been shown that using a truncation cut in the nozzle exit plane additionally to the criterion B, allows a significant reduction of the computational cost with a negligible deviation of the results. B isoline in 0.05 to 0.2 range ensures accurate results. In the present paper, hybrid simulations are realized with $B = 0.1$ isoline, as figure 4 shows. Along the isoline, the probability density

DOI: 10.13009/EUCASS2022-7245

function of particle velocity remains close enough to a Maxwell-Boltzmann distribution, and the flow is assumed to be at equilibrium.

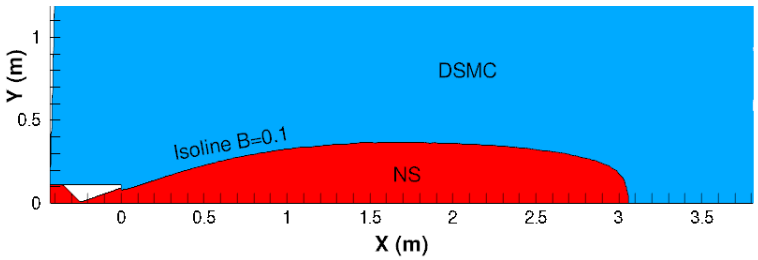

Figure 4: Rarefied and continuous areas of the flow, the interface is defined by $B = 0,1$ isoline from NS simulation

The next step is to translate macroscopic continuous quantities to the probability density function (PDF) of particle velocity used as the unknown variable during DSMC calculation. For this purpose, the isoline is divided into discrete segments. These segments act as inflow boundary conditions for the DSMC simulation, emitting particles according to each segment PDF. As mentioned above, the local thermodynamic equilibrium is assumed along the isoline, and Maxwellian functions are used to describe the PDF according to extracted values of velocity, density and temperature. Taking into account the velocity gradient, a total variation method is used to provide a representative flow with a minimal number of discrete segments as in [15]. This ensures a well-discretised isoline over the flow, in the plume as well as in close range to the wall, to provide DSMC with accurate inflow boundary conditions.

2.4 Direct Simulation Monte Carlo calculation

A DSMC simulation is performed over the rarefied area. It employs numerical particles, representing a large number of physical particles, and describes their behaviour by successively computing their motions and collisions within each time step. More precisely, particle trajectories are first computed according to their velocity regardless of possible intersections. Then, collisions are resolved between nearby particles on a stochastic approach. The macroscopic quantities such as temperature or velocity can be obtained by averaging over many time steps. Accurate simulation relies on three criteria: the time step has to be less than the average time between particle collision to ensure correct particle trajectory computation, the spatial resolution has to be of the order of a particle's mean free path so that collision partners are precisely determined, and the number of particles per cell has to be high enough to keep the statistical scattering low (i.e. at least 10 to 20 particles per cells).

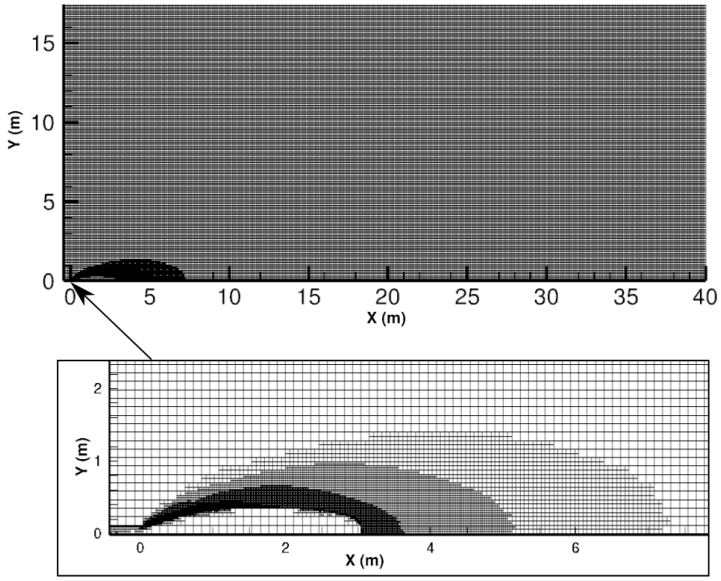

Figure 5: DSMC simulation mesh using a eight levels refinement adaptation method according to the value of the numerical Knudsen number $K_{n,num} = \lambda/\Delta x$, where λ is the particles mean free path, and Δx the cell size

DOI: 10.13009/EUCASS2022-7245

The DSMC tool used for the simulations of this paper is SPARTA [27], an open-source code developed by Sandia National Laboratories. Simulations are realised using the Variable Soft Sphere (VSS) collisional model [28]. Particles-wall interactions are modelled by a Maxwell wall condition with an accommodation coefficient of 1.0. The size of the simulation domain is the same as the NS simulation, and an axial symmetry is also used. The mesh is composed of rectangles defined by 350 points over the x (axial) direction and 150 points over y (radial). The mesh is automatically refined during the simulation according to the value of the numerical Knudsen number $K_{n,num} = \lambda/\Delta x$, λ being the particles mean free path, and Δx the cell size. Figure 5 shows the final mesh obtained with a maximum of eight refinement levels leading to approximately 75000 cells. The cell size ensures a spatial resolution matching the particle mean free path in high-pressure regions. The time step is set to 10^{-7} s, which is less than the average particle collision time in the densest area of the flow. The number of particles per cell is more than 20 for the majority of the simulated species. The simulation convergence is obtained when the total number of particles reaches a steady-state, which is approximately 1.2 billion particles over the simulation domain after 200000 time steps.

2.5 Lagrangian chemical post-computation

The previous steps of the methodology gave the aerodynamic solution taking into account the transition between a continuous and a rarefied flow. This section describes the Lagrangian chemical reactor LARSEN [18] used to compute the plasma over the flow solution. LARSEN computes detailed thermochemical effects along a steady baseline flow simulation streamline. The solver can simulate both continuous and rarefied flows considering thermochemical nonequilibrium via multi-temperature or state-to-state models. Using a Lagrangian chemical post-computation solver allows to decouple the flow and the chemistry simulation to include detailed thermochemical effects into a lower-fidelity baseline solution.

In the present paper, LARSEN enables applying detailed reactional mechanisms and considering minor species in the mixture, which is difficult to handle with DSMC. LARSEN approach needs a baseline solution to extract the velocity and total density fields along its streamlines. Then, a more detailed thermochemical state of the flow can be obtained by re-processing the baseline calculation using more species and chemical reactions. The velocity and density fields are not recomputed, and initial conditions for flow temperature and species concentration are picked at the beginning of the streamlines. The species mass conservation and enthalpy equations are solved along the streamlines in Lagrangian form. The space integration is performed using an adaptative Runge-Kutta 4-5 scheme from the C++ Boost library. The baseline density and velocity values are linearly interpolated as the integrator moves from one streamline point to the next. The physicochemical properties are given by the open-source Mutation++ library [29]. It is assumed that considering minor species and related reactions, extending from the reduced chemistry to the full chemistry, has a neglectable effect on the velocity and density fields of the flow solution, given the insignificant mass, momentum and energy that minor species represent. Furthermore, mass diffusion from a streamline to another is not taken into account, and the new solution is integrated along every streamline separately. This approach is assumed to be valid as the flow velocity is highly supersonic in the axial direction.

LARSEN's ability to compute accurately species concentrations was verified using a simple one-meter-long 1D channel test case of 1000 cells. NS simulations of the channel using full and reduced chemistry were performed for three different conditions given in table 3. These conditions reproduce three thermodynamic states locally encountered in the nozzle as the flow transit from the combustion chamber to the nozzle exit. The same initial species mass fractions are used for the simulation of the three conditions, which are the one listed in table 1. Flow solutions obtained with the full chemistry are considered as reference solutions. Temperature, major species H_2, CO, HCl, H_2O and electron mole fraction post-computed with LARSEN along the channel from the three NS simulations using both full and reduced chemistry baselines are confronted in figure 6. LARSEN results are displayed with dashed lines and NS with solid lines. Re-computation of the temperature and species concentration is highly accurate for the three inlet conditions. If LARSEN computation from NS full chemistry simulation is expected to give identical results, the ones obtained from reduced chemistry are quasi-identical even for the electron mole fraction involving very low fractions.

This gives confidence in the chemical post-computation methodology of the complex kinetic scheme from a reduced kinetic scheme flow solution of the nozzle. Furthermore, the chemistry in the channel flow seems frozen for

Case	T_{inlet} (K)	P_{inlet} (Pa)	P_{outlet} (Pa)
1	100	1	0.9
2	500	100	90
3	2000	100000	90000

Table 3: Channel stream boundary conditions

DOI: 10.13009/EUCASS2022-7245

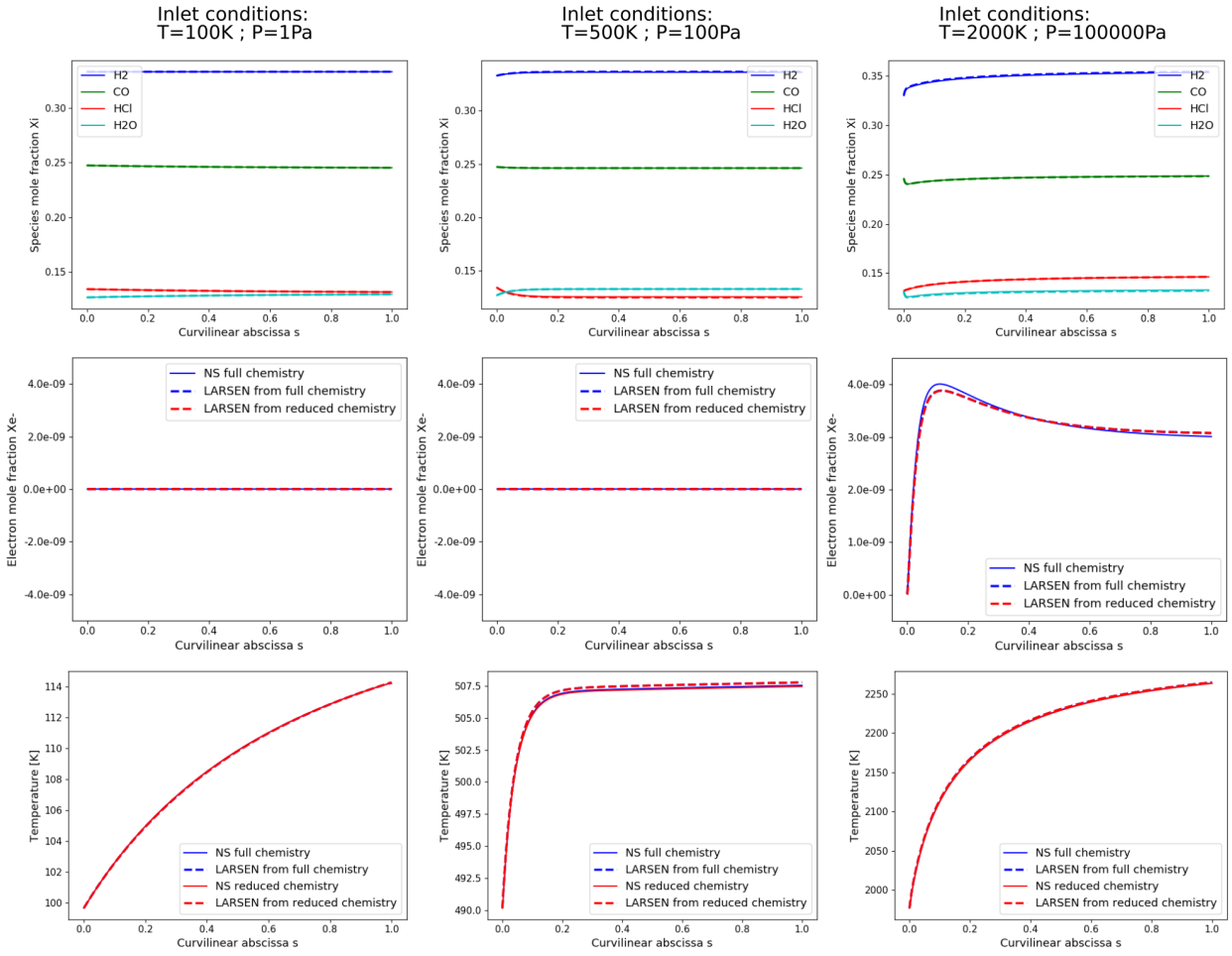

Figure 6: Confrontation of temperature, H_2, CO, HCl, H_2O major species and electron mole fractions between channel full chemistry NS simulations for the three inlet conditions and LARSEN post-computations from full and reduced chemistry NS baseline solutions

temperature less than 500 K and pressure less than 100 Pa. For these conditions, the temperature does not increase significantly, there is no ionization of the flow and the electron mole fraction remains null, which validates our approach to assume negligible the chemical reactions in DSMC simulation of the rarefied part of the flow.

LARSEN is then used in the same way along the nozzle flow streamlines. Figure 7 presents the 59 streamlines used to model the plasma in the nozzle plume. They were obtained by drawing one streamline per metre along the right and top simulation boundaries. Lagrangian chemical re-computing is applied along each of these streamlines to obtain the species mole fraction. The electron density field is then processed by projecting the streamlines data on a cartesian grid, defined by 350 points in the axial direction and 150 in the radial one.

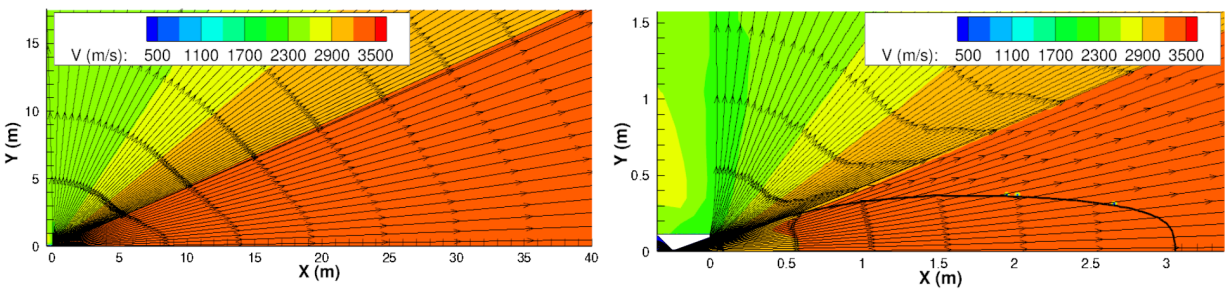

Figure 7: Full domain (left) and close nozzle (right) views of the hybrid flow velocity solution and the 59 streamlines used to model the plasma with LARSEN

DOI: 10.13009/EUCASS2022-7245

3. Simulation results

This section presents the nozzle simulation results obtained with a simple NS computation and with the hybrid methodology described in section 2. The simple NS calculation is performed using the full table 2 chemical scheme, whereas the hybrid NS-DSMC simulation post-computes the full chemistry from a baseline flow solution obtained with a reduced chemical scheme. Figure 8 shows the velocity field obtained with both approaches. The flow resulting from hybrid simulation is widely expanded, which is not the case with the continuous approach as observed in [15]. This could explain the deviation observed by Kinefuchi *et al.* [14] between their simulation results and the flight data occurring for M-V rocket at 183 km flight altitude. Their simulations do not consider the flow rarefaction, and their results underestimate the communication attenuation look angle, which is in accordance with the narrowed plume obtained using a simple NS simulation. The use of a hybrid methodology should improve the prediction of communication attenuation at high flight altitude.

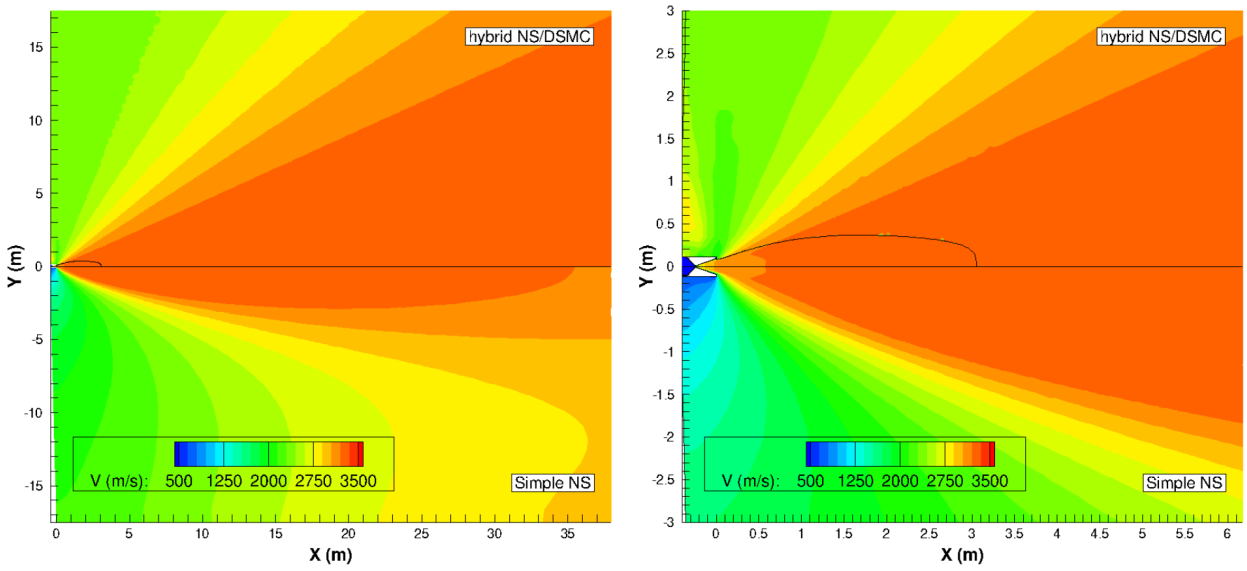

Figure 8: Full domain (left) and close nozzle (right) views of the velocity fields obtained with the hybrid NS-DSMC methodology (top) and with a simple NS simulation (bottom)

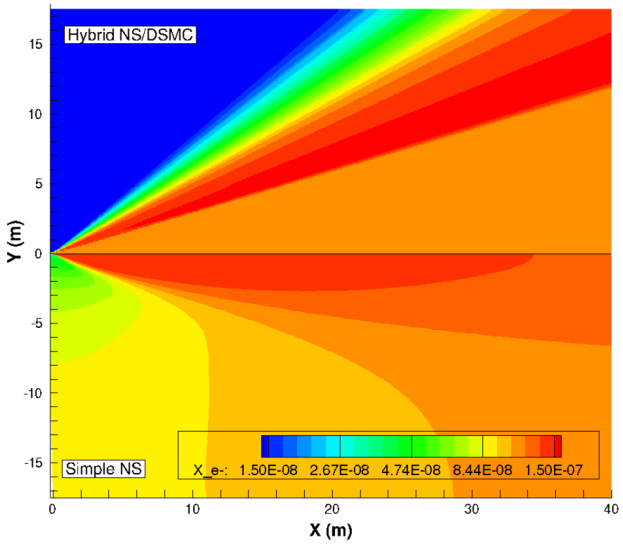

Figure 9: Electron mole fraction field obtained with the hybrid NS-DSMC methodology (top) and with a simple NS simulation (bottom)

Figure 9 presents the confrontation between the electron mole fraction X_{e^-} fields obtained with the two ap-

DOI: 10.13009/EUCASS2022-7245

proaches. The electron mole fraction has the same magnitude in the two results, especially near the plume axial direction, which is the denser part of the flow. However, the flow behavior difference due to rarefaction effects leads to significant changes, particularly in the high look angle area where electron mole fraction level remains above a plateau value according to the NS simulation, but continuously decreases in the hybrid result. Furthermore, X_{e^-} maximum is not obtained along the axial direction in the hybrid simulation but for approximately a 15° angle. These observations are in accordance with the electron density n_{e^-} angular profiles extracted along 5 m and 15 m radius circles around the nozzle, where n_{e^-} is calculated as:

$$n_{e^-} = X_{e^-}\frac{N}{V} = X_{e^-}\frac{p}{k_B T} \tag{3}$$

with X_{e-} the electron mole fraction, N the number of total particles in the volume V, and k_B the Boltzmann constant. Figure 10 presents the n_{e^-} angular profiles extracted from the simulations. NS simulation shows a plateau value at high look angles for both 5 and 15 m profiles. The difference between NS and hybrid simulation results increases with the distance to the nozzle as the hybrid flow continuously expands. As expected, the results are of the same magnitude for both approaches regarding low look angles. The simulations realized in this paper do not consider any co-flow, which should increase the difference of n_{e^-} along the angular profil: in NS simulation, the co-flow would be responsible for electron blowing in the high look angle area, leading to a sharper decrease of the electron density before the plateau value observed in figure 10. On the other hand, the co-flow influence decreases when the altitude increases (hence when the rarefaction of the flow increases), which is modelled using DSMC. This ensures more accurate predictions with the hybrid methodology.

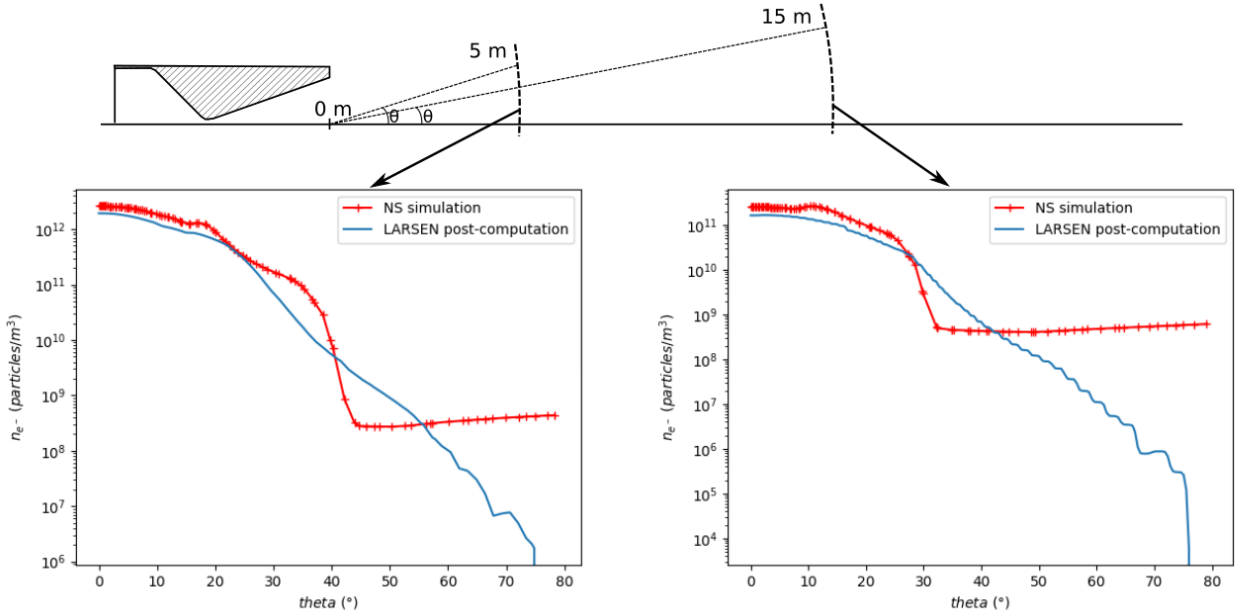

Figure 10: Angular profiles of the electron density n_{e^-} obtained with the simple NS simulation and with the hybrid methodology (LARSEN post-computation) along a 5 m radius cercle (left) and a 15 m radius cercle (right) around the nozzle

Finally, the electron density obtained with the hybrid methodology seems in better agreement with the expectation due to the consideration of the flow rarefaction. However, a comparison with experimental data is necessary to properly validate the methodology. For example, in this paper, the post-computation of the species along the streamlines is realized without accounting for mass diffusion as the flow is highly supersonic. This assumption, and more generally the effect of the flow interaction with the nozzle wall has to be verified. Figure 11 gives the velocity and the electron density along two radius inside the nozzle, one at the divergent mid position and one at the exit. For comparison purposes, the electron density post-computation with LARSEN is directly based on the NS full chemistry simulation as the flow inside the nozzle is dense enough to compute the correct flow behavior with a continuous approach. This ensure that the deviation of the results does not come from the chemistry as LARSEN post-computes the chemistry on a baseline solution that already considers the full reaction scheme. The nozzle divergent boundary layer is a pseudo-rarefied area, and the flow rarefaction leads to bounces on wall temperature and velocity. The bounces increase as the flow exits the nozzle. As figure 11 shows, the velocity decreases to a subsonic level close to the wall but is

DOI: 10.13009/EUCASS2022-7245

still higher than 100 m/s at the mid divergent position, which seems high enough to neglect diffusive effects. However, the streamlines start at the chamber's inlet, where the velocity has value below 30 m/s. Streamlines are initialized with species concentration taken at their start point and no longer interact with the flow solution except for the velocity and total density. Hence, mass diffusion or wall interactions are not considered. Furthermore, in our simulations, the inner nozzle wall is modelled as an isothermal wall with a temperature of 2000 K, which lead to a thermal gradient close to the wall, impacting the streamlines' enthalpy. These effects might not be negligible, which explains the differences obtained for the electron density curves of figure 11. Three blue curves representing the electron density along the two radius are plotted, corresponding to the NS simulation and to its LARSEN re-computation with different start points for the streamline: one at the chamber's inlet, and the other one at the nozzle throat. LARSEN results close to the wall are in better agreement with the NS simulation when streamlines are initialized at the nozzle throat. The influence of the chamber wall interaction on the species concentration is then avoided, which demonstrates the influence of wall interactions. It is shown in our previous work [15] that the inner divergent boundary layer area is responsible for the high look angle particle density, which is of great interest for radio communication issues. The results of the hybrid methodology can be improved considering mass diffusion among streamlines and wall thermal influence in the post-computation of the full chemical scheme.

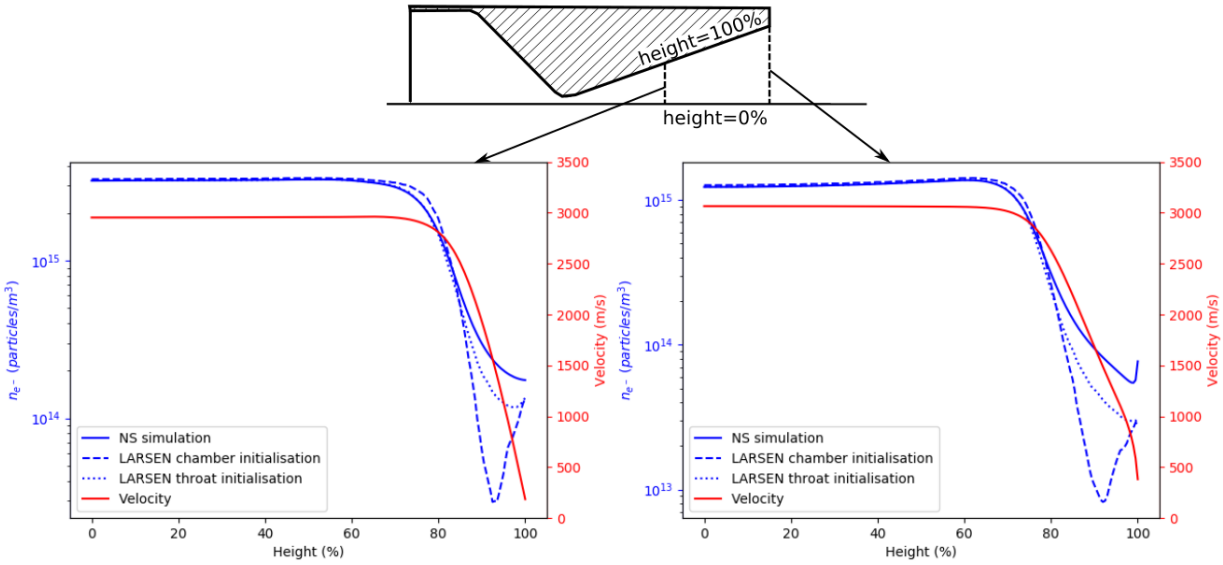

Figure 11: Electron density n_{e^-} obtained with the NS full chemistry simulation and with its LARSEN post-computation along a radius at the divergent mid position (left) and at the nozzle exit (right)

4. Conclusion

In this paper, simulations of highly pressurized thruster ionized flow in a rarefied atmosphere were realized. A methodology is proposed to obtain the electron density field accounting for the effect of atmosphere rarefaction coupling NS and DSMC to handle both continuous and rarefied flow areas. Once the flow solution is obtained, the plasma is post-computed assuming negligible effect of the minor species and ionization reactions on the flow behavior, which is verified on a simple 1D channel test case. In consequence, the full thermochemical calculation is decoupled from the flowfield simulation. Complex chemistry and multiple species that compose a plasma can be post-computed with this approach without increasing the computational time. In the context of this study, this methodology is necessary since electrons and ions are difficult to handle in a DSMC simulation, and their very low concentration level would lead to severe computational constraint due to the statistical convergence. The methodology presented in this work allows to compute the electron density field successfully in a reasonable computational time and the results demonstrates its ability to calculate the plasma flow exhausted from a highly pressurized thruster in a rarefied atmosphere. The results show that the atmosphere's rarefaction significantly influences the flow behaviour, notably in agreement with the expectation of Kinefuchi *et al.*. It is mandatory to consider the flow's rarefaction for thrusters simulation evolving above an altitude of 200 km. Comparison with experimental data remains however necessary to validate properly the methodology regarding the hypothesis it relies on. Quantifying the influence of species mass diffusion and thermal boundary layer in the chamber and the nozzle divergent is important, especially close to the wall. Furthermore, the

DOI: 10.13009/EUCASS2022-7245

chemistry is assumed to be frozen during DSMC simulation. This should also be investigated since the length scale of the plume can reach hundreds of meters in industrial rocket configurations, and chemical reactions might influence the baseline solution from which LARSEN post-computes the final species concentration. The methodology calculation time is ensured to remain acceptable as only reduced chemistry scheme and number of species are considered for the NS and DSMC simulation. With the same idea, it would be interesting to evaluate the use of an inert equivalent gas as the baseline solution, characterized by the mean properties of the combustion chamber product.

References

[1] F. La Torre, S. Kenjeres, J.-L. Moerel, and C.R. Kleijn. Hybrid simulations of rarefied supersonic gas flows in micro-nozzles. *Computers and Fluids*, 49(1):312–322, 2011.

[2] M. Ivanov, D. Khotyanovsky, A. Kudryavtsev, P. Vashchenkov, G. Markelov, and A. Schmidt. Numerical Study of Backflow for Nozzle Plumes Expanding into Vacuum. *37th AIAA Thermophysics Conference*, 06 2004.

[3] C. Glass and P. Gnoffo. A 3-D coupled CFD-DSMC solution method with application to the Mars Sample Return Orbiter. 08 2000.

[4] C. Glass and T.J. Horvath. Comparison of a 3D CFD DSMC Solution Methodology With a Wind Tunnel Experiment. *AIP Conference Proceedings*, 663(1):441–448, 2003.

[5] T. Deschenes, H. Alkandry, and I. Boyd. Application of a Modular Particle-Continuum Method to Hypersonic Propulsive Deceleration. *42nd AIAA Thermophysics Conference*, 06 2011.

[6] J. Burt and I. Boyd. Application of a Multiscale Particle Scheme to High Altitude Rocket Exhaust Flows. 01 2009.

[7] J. Marichalar, A. Prisbell, F. Lumpkin, and G. Lebeau. Study of Plume Impingement Effects in the Lunar Lander Environment. *AIP Conference Proceedings*, 1333, 05 2011.

[8] S.S. Xu, Z.N. Wu, Q. Li, and Y.J. Hong. Hybrid continuum/DSMC computation of rocket mode lightcraft flow in near space with high temperature and rarefaction effect. *Computers and Fluids*, 38(7):1394–1404, 2009. Special Issue Dedicated to Professor Alain Lerat on the Occasion of his 60th Birthday.

[9] O. Aktas and N.R. Aluru. A Combined Continuum/DSMC Technique for Multiscale Analysis of Microfluidic Filters. *Journal of Computational Physics*, 178:342–372, 05 2002.

[10] I. D. Boyd and T. R. Deschenes. Hybrid Particle-Continuum Numerical Methods for Aerospace Applications. 2011.

[11] E. Dieudonné, A. Kameni, L. Pichon, and D. Monchaux. Radio frequency attenuation by a rocket plume using diffraction theory and finite element modeling. *Acta Astronautica*, 158:334–341, 2019.

[12] B. Sun, K. Xie, L. Shi, M. Yang, B. Yao, and S. Guo. Experimental Investigation on Electromagnetic Waves Transmitting Through Exhaust Plume: From Propagation to Channel Characteristics. *IEEE Transactions on Antennas and Propagation*, PP:1–1, 06 2020.

[13] K. Kinefuchi, K. Okita, I. Funaki, and T. Abe. Prediction of In-Flight Radio Frequency Attenuation by a Rocket Plume. *Journal of Spacecraft and Rockets*, 52(2):340–349, 2015.

[14] K. Kinefuchi, H. Yamaguchi, M. Minami, K. Okita, and T. Abe. In-flight S-band telemetry attenuation by ionized solid rocket motor plumes at high altitude. *Acta Astronautica*, 165:373–381, 2019.

[15] V. Charton, A. Awad, and J. Labaune. Optimisation of a hybrid NS-DSMC methodology for continuous-rarefied jet flows. *Acta Astronautica*, 195:295–308, 2022.

[16] M. Grabe, S. Fasoulas, and K. Hannemann. *Numerical Simulation of Nozzle Flow into High Vacuum Using Kinetic and Continuum Approaches*, volume 112, pages 423–430. 05 2010.

[17] M. Grabe, G. Dettleff, and K. Hannemann. Comparison of Computed Free Thruster Plume Expansion to Experiments. 05 2014.

DOI: 10.13009/EUCASS2022-7245

[18] S. Boccelli, F. Bariselli, B. Dias, and T.E. Magin. Lagrangian diffusive reactor for detailed thermochemical computations of plasma flows. *Plasma Sources Science and Technology*, 28(6):065002, may 2019.

[19] A.L. Garcia and B.J. Alder. Generation of the Chapman-Enskog Distribution. *J. Comput. Phys.*, 140(1):66–70, February 1998.

[20] JAXA Special Publication. *JAXA-SP-07-023*, 2008.

[21] J. Troyes, I. Dubois, V. Borie, and A. Boischot. *Multi-Phase Reactive Numerical Simulations of a Model Solid Rocket Exhaust Jet*.

[22] D.E. Jensen and P.J. Padley. Kinetic studies of ionization and recombination processes of metallic additives to flames. *Symposium (International) on Combustion*, 11(1):351–358, 1967.

[23] D.E. Jensen and G.A. Jones. Reaction rate coefficients for flame calculations. *Combustion and Flame*, 32:1–34, 1978.

[24] John M. C. Plane, B. Rajasekhar, and Libero Bartolotti. An experimental and theoretical study of the reactions Na+HCl and Na+DCl. *The Journal of Chemical Physics*, 91(10):6177–6186, 1989.

[25] A. Refloch, B. Courbet, A. Murrone, P. Villedieu, C. Laurent, P. Gilbank, J. Troyes, L. Tessé, G. Chaineray, J.B. Dargaud, E. Quémerais, and F. Vuillot. CEDRE Software. *Aerospace Lab*, (2):p. 1–10, March 2011.

[26] M. Smoluchowski von Smolan. Ueber WÃd'rmeleitung in verdÃijnnten Gasen. *Annalen der Physik*, 300(1):101–130, 1898.

[27] S. J. Plimpton, S. G. Moore, A. Borner, A. K. Stagg, T. P. Koehler, J. R. Torczynski, and M. A. Gallis. Direct simulation Monte Carlo on petaflop supercomputers and beyond. *Physics of Fluids*, 31(8):086101, 2019.

[28] I.D. Boyd and T.E. Schwartzentruber. *Nonequilibrium Gas Dynamics and Molecular Simulation*. Cambridge Aerospace Series. Cambridge University Press, 2017.

[29] James B. Scoggins, Vincent Leroy, Georgios Bellas-Chatzigeorgis, Bruno Dias, and Thierry E. Magin. Mutation++: MUlticomponent Thermodynamic And Transport properties for IONized gases in C++. *SoftwareX*, 12:100575, 2020.